In situ detection of Microplastics: Single Microparticle-Electrode Impacts

*Kenichi Shimizu[a]†, Stanislav V. Sokolov 1†, Enno Kätelhön[a], Jennifer Holter[b], Neil P. Young[b], Richard G. Compton[a]**

[a] 1Department of Chemistry, Physical and Theoretical Chemistry Laboratory, Oxford University, South Parks Road, Oxford, OX1 3QZ, United Kingdom

[b] Department of Materials, Oxford University, Parks Road, OX1 3PH, United Kingdom

† Both authors contributed equally

* e-mail: richard.compton@chem.ox.ac.uk

Received: ((will be filled in by the editorial sttaff))
Accepted: ((will be filled in by the editorial sttaff))

Abstract

Particle-impact electrochemistry is employed to study spherical polyethylene microparticles suspended in an aqueous solution. This electrochemical method detects polyethylene microparticles impacting on a carbon fiber electrode generating a transient current response or “spike”. We interpret the physio-chemical origin of the spikes and accurately identify particle size distributions and concentrations for microparticles of sizes 1–10 μm.

Keywords: Microplastics; electrochemical detection; particle-electrode impacts; chronoamperometry

DOI: 10.1002/elan.((will be filled in by the editorial sttaff))

1. Introduction

The particle-electrode impact method has been widely and diversely applied to study nanoparticles suspended in aqueous solution. Fundamental aspects and potential applications have been reviewed previously.[1–6] The technique involves a conventional three-electrode setup for an electrochemical analysis with a working electrode held at a suitable potential to observe an electrochemical reaction at, or of, individual particles that are suspended in an aqueous or other solutions such as ionic liquids.[7] Collisions of the particles with the electrode occur by virtue of their Brownian motion which may result in a charge transfer between the colliding particle and the stationary electrode. This can be due to either Faradaic (charge crosses the electrode-solution interface) or non-Faradaic (capacitive) processes depending on the applied potential and physicochemical properties of colliding particles. Such processes are recorded as transient current signals or spikes in a chronoamperogram. In the case of Faradaic collision, which may involve reaction of the particle (for example dissolution of an impacting silver nanoparticle[8] , reduction of hematite particles[9]) or mediated reaction at the particle (proton reduction on impacting Pt nanoparticle[10]), through analysis of spikes or steps the information regarding the size and physicochemical properties of the impacting particle can be extracted.[5,8,10,11] The method is also applicable to characterizing Faradaically inert conductive particles as demonstrated in a study which determined the potential of zero charge of graphene platelets and complements the use of cyclic voltammetry in such cases.[12,13] The present work is concerned with the detection and *physio-chemical aspects* of collisions of electrically insulating micro-particles.

Specifically we study collisions resulting from suspension of small insulating polyethylene particles in aqueous electrolyte. In this case there is no possibility of direct Faradaic electron transfer to and from the polyethylene particles themselves due to the fact that polyethylene is an insulator. Nevertheless as will be reported, current transients ('spikes') correlated with the impacts were observed. An initial aim of the present paper is to explore the physiochemical origin of these spikes. In addition electrode-particle impacts may be a potential tool for environmental detection of microplastics given the particular concern in recent years due to unknown dangers to aquatic environment and the associated human health hazards, [14–16] since the frequency of the impacts is shown to scale directly with the particle concentration.

2. Experimental

2.1. Chemicals and Materials

Three distinct size groups (1-4 μm, 3-16 μm, and 10-22 μm in diameter) of spherical polyethylene microparticles were purchased from Cospheric (density: 0.95 – 0.99 g cm^{-3}, Santa Barbara, USA) and used after dispersion in 20mM sodium chloride solution. Sodium chloride was purchased from Sigma-Aldrich (≥ 99.0 %, Steinheim, Germany). Nitrogen gas used to degas the solution was supplied by BOC Gases plc (99.998%, Guildford, UK) and was humidified by passing through traps of ultrapure water and 0.1 M NaOH. A glassy carbon macro electrode (3.0 mm in diameter) and a saturated calomel reference electrode (saturated KCl, SCE, 0.242 V *vs.* normal hydrogen electrode) were purchased from ALS Co. Ltd. (Tokyo, Japan). The glassy carbon working electrode was polished to a mirror finish prior to the use on aqueous slurries of 1, 0.3, and 0.05 μm alumina in descending order of size. Thereafter, in order to remove alumina residue, the electrode surface was rinsed with excess ultrapure water and wiped with a wet

tissue. A platinum wire used as a counter electrode was purchased from Goodfellow Cambridge Ltd. (Huntington, UK). Carbon fiber micro-wire electrodes (7.0 µm in diameter, approximately 1 mm in length) were prepared in-house according to a method described previously.[17] Briefly, the micro-wire electrode was fabricated in the following manner: single carbon fiber (XAS grade, Goodfellow Cambridge Ltd.) was first attached to the tip of a silver wire using a silver loaded epoxy (RS Components Ltd., Northants, UK). The epoxy was then dried in an oven at 60 °C for 15 min. The wire was thereafter inserted through a 200 µL pipette tip (VWR International Ltd., Lutterworth, UK). The carbon fiber/silver wire connection and the pipette tip was sealed using cyanoacrylate adhesive (Grade 102, Permabond Engineering Adhesives Ltd., Common, UK). Finally, carbon fiber was cut to the length of approximately 1 mm using a scalpel. The micro-wire electrodes were briefly sonicated for 5 s in ultrapure water prior to use.

2.2. Physical characterization of small polyethylene microparticles

The morphology and shape of polyethylene microparticles used in this work was examined by scanning electron microscopy (SEM) using a Zeiss Evo MA10 microscope with an accelerating voltage of 10 kV using secondary electron imaging mode. For SEM imaging, the particles pre-dispersed in ultrapure water were pipetted onto a glassy carbon substrate and dried under ambient condition. Subsequently the samples were coated with gold film to provide sufficient electrical conductivity which is important to reduce the imaging artefacts. Optical microscopy was performed using bright field imaging mode with a Zeiss Axio Examiner.A1 equipped with an air objective with 20 x magnification.

The size measurement of microparticles was carried out using ImageJ software (v. 1.51a, imagej.nih.gov/ij/) and size distributions were determined using Origin Pro 2015 software (OriginLab Co., Northampton, USA) under the assumption of spherical geometry. Zeta potentials of microspheres suspended in 20 mM NaCl were analyzed using Zetasizer Nano ZS (Malvern Instruments, Ltd. Malvern, UK) equipped with a 638 nm laser source. Pre-dispersed particles were introduced into the folded capillary cell using a disposable syringe. Measurements were repeated six times during which the suspension was re-dispersed by brief ultrasonic agitation.

2.3. Electrochemical analysis

All electrochemical experiments were conducted using a conventional three-electrode setup in a Faraday cage while the electrochemical cell was kept under a N_2 atmosphere and the temperature maintained at 25 °C. Measurements were made using a Metrohm µAutolab II potentiostat (Utrecht, the Netherland) with Nova (v.1.11.2) as an operating interface. The charge measured in this way resulting from a particle-electrode collision is fully conserved in the current transients recorded using the potentiostat despite possible distortion of the current-time response as validated previously in the literature.[18,19]

For cyclic voltammetric analysis, a 4 µL aliquot of micro-plastic spheres dispersed in ultrapure water was placed onto the surface of glassy carbon electrode and dried under ambient condition. The amount of the microplastic spheres deposited was 0.28 mg cm^{-2} or equivalent to the average of two close-packed monolayers on the working electrode. Once dried, the modified electrode was thoroughly rinsed with ultrapure water and placed in a deoxygenated 20 mM NaCl. The potential was swept between 1.0 V and -1.0 V vs. SCE at the scan rate of 0.010 V s^{-1}.

Particle-impact chronoamperometry was conducted using the in-house prepared carbon fiber micro-wire electrode as a working electrode.[17] Chronoamperograms were recorded for the duration of 50 s with a 0.5 ms measurement interval at the bias potential of between -1.0 V and 0.8 V vs. SCE. The dispersion of the polyethylene microspheres in 20 mM NaCl solution was achieved by sonicating the electrochemical cell for 10 s every 2-4 measurements. The need for this is illustrated by optical microscopy imaging using the large particles (10-22 µm) which demonstrated the sticking of the particles to the carbon fiber within ca 60 s after the particles were introduced into the cell. The resultant images are shown in Figure 1 and clearly demonstrate the adsorbed particles on the electrode surface. This observation suggests adsorption of particles to the electrode upon impact and sonication allows re-suspension of the adsorbed particles.

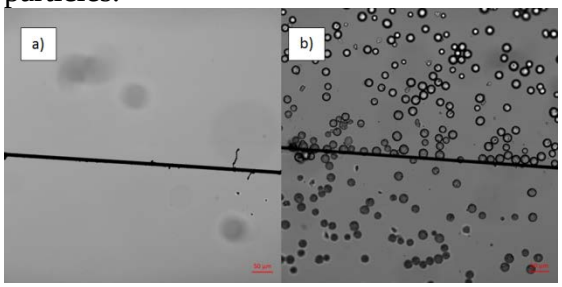

Figure 4: Optical microscopy images of the carbon fiber electrode (a) in the absence of microparticles, (b) after 60 s of introduction of microparticles to the chamber

Transient current responses or "spikes" resulting from microparticles colliding with the micro-wire electrode were analyzed using Signal Counter software [20] and the impact charge distributions were calculated using Origin 2015 software.

3. Results and Discussion

In the following sections we first examine the morphology (size and shape) of the particles using scanning electron and optical microscopy. Then we report the zeta potential of micro-plastics and their colloidal stability. Possible electroactivity of the microparticles is subsequently assessed via cyclic voltammetry. Thereafter, particle-impact chronoamperometry is conducted for the detection of the micro-plastics. We discuss the nature of the observed impacts and the importance of the observed spike shape.

3.1. Physical characterization of micro-plastics

The morphologies of polyethylene microspheres in three different size groups as supplied by the manufacturer (1-4 µm, 3-16 µm, and 10-22 µm in diameter) are shown in Figure 2. Images of the smaller two size groups were captured using a scanning electron microscope whereas that of the largest size group was taken with an optical microscope. The diameters of the near-spherical particles captured in the microscopic images were determined using ImageJ software and are summarized in the histograms (Figure 2), least square fitting was used for the Gaussian curves. It was found that the mean diameter of the smallest size group is 2.3 (± 1.1) µm after 87 individual particles were measured. The mean diameters of the medium size and the large size groups are 4.9 (± 1.1) µm and 19.8 (± 3.8) µm, respectively. These results were in good agreement with the manufacturers' specifications and the particles were used for subsequent electrochemical experiments.

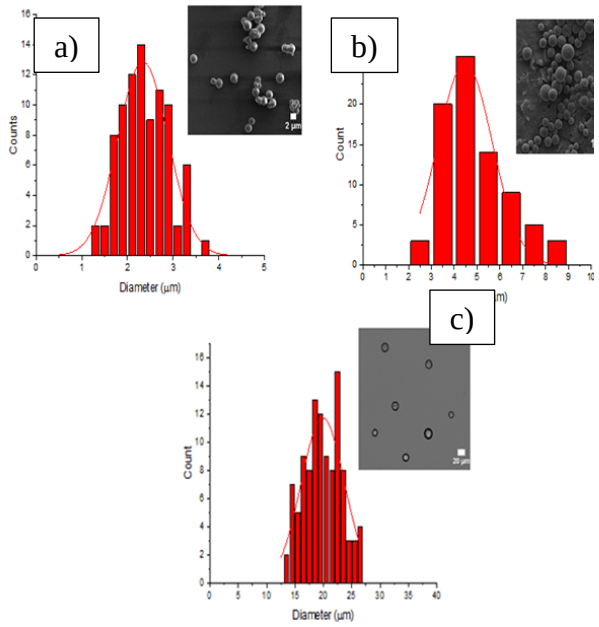

Figure 2: Size distributions of spherical polyethylene microparticles of a) 1-4 µm size, inset SEM image of the particles, b) 3-16 µm size, inset SEM image of the particles c) 10-22 µm size, inset optical microscopy image of the particles

In order to assess the likely colloidal stability of the polymer microparticles in the electrolyte solution, zeta potential measurements were performed. The resultant zeta potentials are shown in Table 1 for the three different ranges of microparticles assessed according to size. The zeta potential was negative for all particle size ranges. This indicates that the surface of the particles is negatively charged. This observation is consistent with previous literature reports which state that the although bulk polyethylene itself is neutral, the charge may arise due to: (i) surface impurities due to manufacturing procedure, (ii) specific adsorption of anions, (iii) hydroxyl ion adsorption.[21] It is found that the polyethylene microparticles of all size groups are negatively charged in 20 mM NaCl solution with a magnitude of greater than 20 mV. This is generally considered a requirement for the stability of a colloidal suspension.[22] Nevertheless, for large particles, slow flotation of particles was observed after tens of seconds. In comparison, the particles in the smallest size group, which showed the most negative zeta potential value of -50.8 (± 10.0) mV, formed the most stable colloidal suspension.

Particle diameter range (d)	E_{Zeta} (mV)
1 – 4 µm	-50.8 ± 10
3 – 16 µm	-27.8 ± 8
10 – 22 µm	-25.8 ± 10

Table 1: Zeta potential (E_{zeta}) measurements for the three size groups of polyethylene microparticles used in the present work

3.1. Cyclic voltammetric characterization of microplastics

It is important to clarify any *intrinsic* electrochemical activity of microparticles in order to successfully design the particle-impact experiment. A survey of possible electrochemical activity of the micro-plastics was initially conducted by cyclic voltammetry. Plastic particles were first drop-cast onto a glassy carbon electrode (surface area of 0.071 cm^{-2}) with the surface coverage of 0.28 mg cm^{-2} or approximately equivalent to the average thickness of two monolayers. Thereafter the modified electrode was placed in 20 mM NaCl solution and the potential was cycled between +1.0 V and -1.0 V vs. SCE at the rate of 0.010 V s^{-1} while recording the current generated at the working electrode. This experiment was conducted under a N_2 atmosphere and the solution was de-oxygenated prior to the measurement in order to avoid oxygen reduction reaction which takes place at a glassy carbon electrode at a potential near -0.40 V vs. SCE in pH neutral media[23] and was repeated using a bare glassy carbon electrode for comparison. The resulting voltage-current curves are shown in Figure 3. The voltammogram of the bare electrode, which is indicated by the red line, shows the capacitative response of the macroelectrode. The voltammetric response of modified electrode, which indicated by the blue line, shows almost identical result to that of the bare electrode

suggesting that polyethylene microparticles are *intrinsically* electrochemically inert in the applied potential region. However it is important to consider the effect of the background capacitance in the voltammogram which arises due to double layer charging and will be proportional to the area of an electrode. The magnitude of the capacitative current (i_{cap}) is given by Equation 1.[24–26]

$$i_{cap} = 2ACv$$

where A is the area of an electrode (m^2), C is the electrode capacitance ($\mu F\ m^{-1}$) and v is the scan rate ($V\ s^{-1}$). The glassy carbon electrode used in the present work has macroscopic dimensions (r=1.5 mm) and as a result low-magnitude Faradaic currents from the particles can be obscured by this large capacitative response. As a result the chronoamperometry based electrode-impact method can be advantageous as the double layer charging effects are minimized and charge transfer resulting from the collision of individual microparticles can be detected.

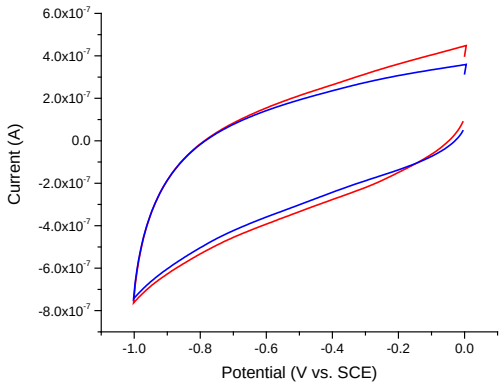

Figure 2: Cyclic voltammograms of (red) bare and (blue) micro-plastic modified glassy carbon electrode recorded in de-oxygenated 20mM NaCl solution at the scan rate of 0.01 $V\ s^{-1}$ at 25 °C. The surface coverage of micro-plastics of the small size group was 0.28 $mg\ cm^{-2}$ or approximately equivalent to the average thickness of two monolayers. The arrow indicates the direction of scan, which started at 0 V vs. SCE.

3.2. Detection of micro-plastics by particle-impacts

The electrode-particle impact experiment was first carried out using 0.74 $g\ L^{-1}$ of polyethylene microparticles of the smallest size group suspended in 20 mM KCl as the electrode potential was varied from -0.8 V to +0.0 V vs. SCE. Responses in form of short current spikes were observed at -0.2 V vs. SCE or more negative potentials.

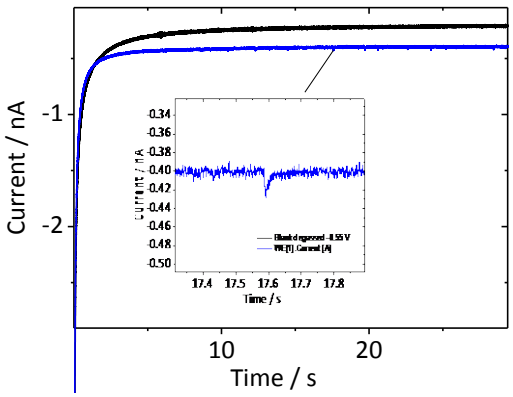

Figure 4. Characteristic chronoamperogram recorded in deoxygenated aqueous suspension of the polyethylene microparticles in 20 mM NaCl using carbon fiber micro-wire electrode and at an applied potential of -0.5 V vs. SCE (blue line) and a solution in the absence of particles (black line). The inset provides an enlarged view of a transient current-time signal resulting from a collision event.

The magnitude of the charge transferred upon particle-electrode collision is determined by integrating the area under the spike. It has been demonstrated previously that although the spike *shape* would be dependent on the filters used in the potentiostat design, the spike *charge* is conserved and as result individual spikes can be used for charge-based analysis, irrespective of their shape.[19] The distribution of observed integrated charges is revealed by a histogram. Figure 5a shows such histogram of the integrated cathodic charges obtained from the particle-impact measurement carried out at -0.5 V vs. SCE. The mean impact charge as a function of applied potential is depicted in Figure 5b. The figure shows that the magnitude of charges transferred upon impact is roughly constant between -

0.8 V and -0.5 V vs. SCE. No impact responses were observed at potentials between -0.2 V and +0.0 V vs. SCE.

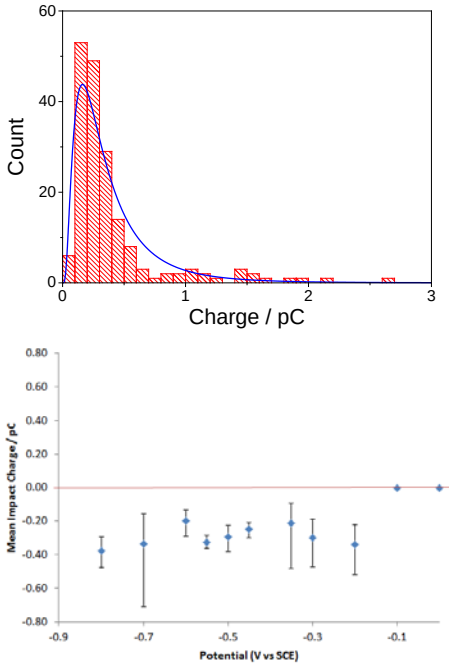

Figure 5 a) Histogram showing the distribution of integrated charges extracted from spikes resulting from chronoamperometric measurements in deoxygenated 20 mM NaCl at -0.5 V vs. SCE using a carbon fiber micro-wire electrode. A total of 187 spikes are analyzed, and the log normal average charge found to be 0.29 (*/ 0.77) pC. b) The log-normal average of charges from polyethylene microparticles as a function of the applied potential. The mean diameter of the particles is 2.3 (± 1.1) µm. Error bars indicate the standard deviations.

3.3. Understanding the nature of the spikes

The cyclic voltammetry analysis above demonstrated that the particles do not show *intrinsic* Faradaic electroactivity on a macroelectrode, yet in the presence of particles exclusively reductive collision events were observed at potentials from -0.80 to -0.20 V vs SCE. It is important to consider the origin of the impacts as it provides important physical insights into the electrode-particle collision. In order to understand the nature of the observed spikes it is important to note that after prolonged degassing (nitrogen bubbling >5 hours) no spikes were observed, while for the normal degassing procedure (nitrogen bubbling ≈ 15 min duration) clear reductive spikes were observable. Hence a potential explanation for the observed reductive reaction based on the potential dependence of the observed spikes and the effect of the degassing is that due to solubility of oxygen in polyethylene an impacting particle can act as an oxygen carrier and upon impact the contained oxygen can be reduced to hydrogen peroxide. The particle itself does not react. The following overall reaction (reaction 1) can take place[27,28]upon impact:

$$O_2 + 2H^+ + 2e^- \rightarrow H_2O_{2_{aq.}} \quad (1)$$

As shown in Figure S4, solution phase oxygen reduction takes place on a bare microwire electrode at a more negative potential in comparison to the potential for spikes in Fig. 5b which is close but more positive than required for the reduction of oxygen in aqueous solution. Since the initial electron transfer is likely due to the oxygen dissolved in the plastic sphere this difference would be due to the stability of $O_2^{-\cdot}$ within the sphere.

If oxygen dissolved in the sphere is the cause of the reductive spike, the magnitude of the spike would be proportional to the amount of dissolved oxygen in a given particle. The estimated maximum theoretical charge transferred per impacting particle based on the assumption of spherical geometry with a radius of 1.15 µm (taken from SEM imaging of the small microparticles used in the present work), solubility of oxygen[29,30] of 0.5×10^{-3} mol/kg , and a 2 electron charge transfer per oxygen molecule[27,28] was 6.1×10^{-13} C. Hydrogen peroxide is the intermediate product and does not get readily reduced at carbon electrode in the potential range employed in this study.[28,31,32] In any case, it is not feasible to detect the reduction of the molecule to water because of the rapid dissipation of the molecule upon completion of Eq. 1 as reported by Neumann et al.[23] A reasonable agreement was observed between the theoretical prediction and experimentally observed mean charge of 3.0×10^{-13} C. The potential

explanation for the discrepancy could be due to the fact that not all oxygen is accessible for the reaction on the timescale of an impact and/or that the particles are incompletely saturated with oxygen. The lack of the faradaic current for the electrochemical reduction of oxygen during the cyclic voltammetric analysis shown in Figure 2 is because the oxygen concentration is too low to generate a significantly large faradaic current response in comparison with the intrinsic capacitive response of the working electrode.

3.3. Analysis of spike shapes

Having established the possible nature of the observed spikes is due to the dissolved oxygen within the particles it is important to consider the factors affecting the observed spike shape. Recent literature has revealed that the analysis of current spikes observed in nano-impacts may also yield important information on the charge transfer mechanism beyond the detection of an impact event and the overall charge transferred.[19,33] The analysis of the measured spike shapes may however be complicated as the employed analogue measurement equipment may drastically alter or even entirely mask the actual spike shape.[1,18] Importantly however, the overall *charge* of the spike is conserved even though the spike shape may be altered drastically[6,15] which for instance has been previously demonstrated for a potentiostat similar to the one used in this study[20]. It is hence crucial to consider the effect of the potentiostat on the measured spike shape.

In order to investigate the information content of measured spike shapes, we have numerically modelled the spike shapes that arise from a signal much faster than the bandwidth of the potentiostat. Subsequent comparison with the measured spikes then reveals whether shape information can be retained from the experimental data or all shape information is removed through bandwidth limitations imposed by the potentiostat. A detailed explanation of the theoretical model is provided in the electronic supplementary material. In short, the analysis first performs an automatic baseline subtraction of the experimental data. Thereafter individual spikes are overlaid with a theoretically-modelled current-time response of the analogue circuitry to a signal that is far too short to enable a recovery after the signal processing of the potentiostat. This theoretical spike features the same integral as the corresponding experimental spike and hence enables a direct comparison between the theoretical model of an entirely bandwidth-limited spike and the actual measurement.

Figure S3 compares the measured spike shapes with the theoretical pulse responses, which is the computationally determined response of the potentiostat to a pulse featuring the length of one sampling interval and the same integral as the measured spike. Since the duration of one sampling interval far exceeds the bandwidth of the potentiostat, the modelled spikes resemble the limiting case of the amplifier's response to a spike that is too fast to be resolved. The figure shows that measured spike shapes are close to the corresponding pulse responses and therefore likely affected by the potentiostat’s bandwidth, though spike onsets are slower and longer tails are observed. While the onsets likely reflect the particles Brownian motion inside the double layer during its approach to the electrode and possibly additional capacitive effects in the measurement equipment, the only slightly longer tails may indicate an actual spike length of the order of the potentiostat’s bandwidth. It is however noted, that our analysis can only consider larger spikes as the experimental data is affected by the bit noise of the potentiostat's analogue-digital converter

masking the smaller ones. In addition we did not observe any 'reverse-spikes' in the oxidative direction, which further suggests that the observed collisions are Faradaic in nature.

3.3. Experimental Charge Distribution and Sizing of the Particles

We believe the impacts to be due to the dissolved oxygen within the particles and as a result provided that oxygen concentration within a particle does not change on the timescale of the experiment other than due to electrolysis by virtue of the impact, we can estimate the size of the impacting particles. If there is full consumption of the oxygen in each impacting sphere, the charge transferred per impact is directly proportional to the concentration of oxygen within a particle and as a result the radius of the particle can be estimated under assumption of spherical geometry and uniform density of a particle.[34] Figure 6 shows the comparison between the size distributions obtained via SEM imaging (μ_{radius}=1.15 µm, σ=0.50) and the calculated radii (μ_{radius}=1.03 µm, σ=0.75) from the impact experiments. Reasonable agreement is observed, thereby allowing the sizing of the impacting particles. A larger standard deviation is observed for the in situ impact experiments in comparison to ex situ electron microscopy which is potentially indicative of the clustered particles being present in the solution during the experiment.

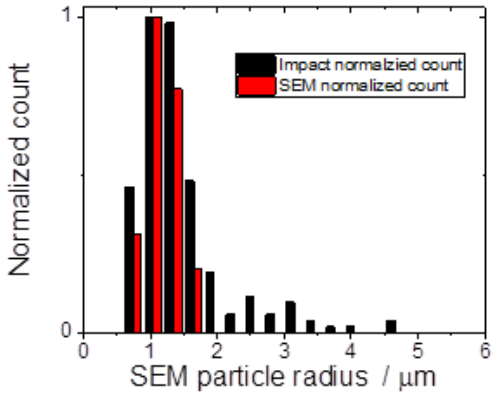

Figure 6: Comparison between the radii distributions obtained via electrode-particle impacts (black bars) and SEM imaging (red bars).

3.4. Impact Frequency

It is desirable for an analytical tool to be able to find the concentration of plastic microparticles in situ. Herein, it is demonstrated that the concentration can be roughly estimated based on the frequency of observed impact events during the particle-impact experiment. The particle-impact experiment was conducted in the 20 mM NaCl solution at the bias potential of -0.5 V vs. SCE with concentration of polyethylene microparticles ranging from 3.6×10^{9} particles L^{-1} to 1.4×10^{11} particles L^{-1}. Eight to 43 chronoamperograms were recorded; a greater number of measurements was needed for the system with lower particle concentrations. Thereafter, the total number of observed cathodic spikes was divided with total measurement time to obtain the collision frequency. It is insightful to compare the experimentally observed number of impacts and the theoretical prediction based on the mass transport of the particles. The theoretical values are derived from the Szabo equation shown below,[17,35,36] considering the collision frequency as function of the dimension of the stationary electrode and diffusion coefficient of the particles in addition to the particle concentration. This expression is derived using the concentration of particles at the electrode

surface to be zero ($c_{elec}=0$). In effect there is a reduction in the local concentration of the oxygenated particles and the concentration of freely diffusing oxygen filled particles at the electrode surface is effectively zero. As a result the modified Szabo expression[17,35] (Eq.1) can be used to estimate the flux (moles m^{-2} s^{-1}) to the electrode surface for the irreversibly adsorbing particles.

$$flux = \frac{DC}{r_0} f(\tau) \quad \text{Eq.1}$$

$$f(\tau) = \frac{2e^{-\frac{\sqrt{\pi\tau}}{20}}}{\sqrt{\pi\tau}} + \frac{1}{\ln\left[(e^{-\gamma\tau})^{0.5} + e^{\frac{5}{3}}\right]}$$

Eq.2

$$\tau = \frac{4Dt}{r_0^2} \quad \text{Eq. 3}$$

$$D = \frac{k_B T}{6\pi\eta r} \quad \text{Eq. 4}$$

where r_0 is the radius of the electrode, C_0 is the concentration, t is the time of the chronomaperogram, γ=0.57721 and is a constant derived from the limits of the Bessel function and D is the diffusion coefficient that is calculated using the Stokes-Einstein-Sutherland[37,38] equation (Eq.4), in which k_b is the Boltzmann constant, T is the temperature, η is the viscosity of the solution and r is the radius of a particle. Figure 7 shows the experimentally obtained collision frequency (indicated by the black square symbols) and theoretical estimates (indicated by red circles) as a function of particle concentrations. Good correlation between the two parameters is observed with the goodness of the fit (R^2) of 0.96 covering approximately three orders of magnitude of particle concentrations. The experimentally obtained collision frequencies however appears to be lower than the theoretically estimated values. The discrepancy could be due to the fact that negatively charged particles are being repelled by an electrode held at a negative potential, which would result in lower probability of collision taking place and as a result lower number of impacts would be observed.

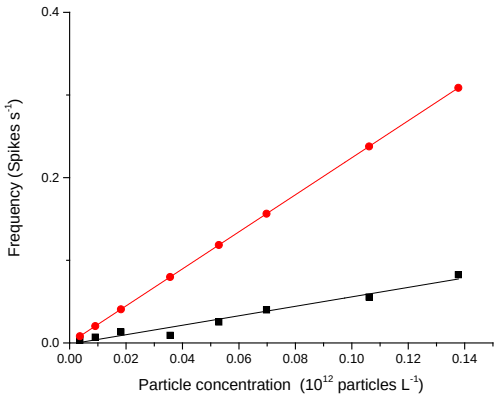

Figure 7: Comparison between the theoretically predicted number of impacts by the Szabo equation (red line) and the experimentally observed frequency (black line).

The results described in the present study are a promising proof-of-concept of the application of the particle-impact technique to study and have potential for fast quantitative size and approximate concentration analysis of micron-sized non-conductive particles.

4. Conclusions

The particle-impact technique has been successfully extended to study collisions of microplastics of variable sizes. The current spikes allow determination of the amount of oxygen carried by an individual impacting particle and also provide information regarding the nature of particle-electrode interaction. The proposed method holds significant advantages over the conventional methods due to high reliability, accuracy and applicability to a wide range of particulate systems. In addition the technique is less affected by polydisperse samples and is clearly capable of detecting wide particle size ranges and could be extended to other types of microparticles. The method is general and can provide further insights into particle-electrode interactions, which are difficult to determine using the conventional techniques.

5. Acknowledgements
This work was supported by a Marie Skłodowska-Curie Intra-European Fellowships (# 626320) (KS) and the European Research Council (FP/2007-2013/ERC Grant Agreement no. [320403]) (SVS, RGC) within the 7th European Community Framework Programme.

6. References

(1) Sokolov, S. V.; Eloul, S.; Kätelhön, E.; Batchelor-McAuley, C.; Compton, R. G.; Cheng, W.; Compton, R. G.; Mirkin, M. V.; Sun, T.; Yu, Y.; et al. Electrode–particle Impacts: A Users Guide. *Phys. Chem. Chem. Phys.* **2017**, *19*, 28–43.

(2) Robbs, P. H.; Rees, N. V. Nanoparticle Electrochemistry. *Phys. Chem. Chem. Phys.* **2016**, *35*, 583–592.

(3) Cheng, W.; Compton, R. G. Electrochemical Detection of Nanoparticles by "nano-Impact" Methods. *TrAC Trends Anal. Chem.* **2014**, *58*, 79–89.

(4) Rees, N. V. Electrochemical Insight from Nanoparticle Collisions with Electrodes: A Mini-Review. *Electrochem. commun.* **2014**, *43*, 83–86.

(5) Pumera, M. Impact Electrochemistry: Measuring Individual Nanoparticles. *ACS Nano* **2014**, *8*, 7555–7558.

(6) Gooding, J. J. Single Entity Electrochemistry Progresses to Cell Counting. *Angew. Chemie Int. Ed.* **2016**, *55*, 12956–12958.

(7) Tanner, E. E. L.; Batchelor-McAuley, C.; Compton, R. G. Single Nanoparticle Detection in Ionic Liquids. *J. Phys. Chem. C* **2016**, *120*, 1959–1965.

(8) Zhou, Y.-G.; Rees, N. V.; Compton, R. G. The Electrochemical Detection and Characterization of Silver Nanoparticles in Aqueous Solution. *Angew. Chemie Int. Ed.* **2011**, *50*, 4219–4221.

(9) Shimizu, K.; Tschulik, K.; Compton, R. G. Exploring the Mineral–water Interface: Reduction and Reaction Kinetics of Single Hematite (α-Fe2O3) Nanoparticles. *Chem. Sci.* **2016**, *7*, 1408–1414.

(10) Xiao, X.; Bard, A. J. Observing Single Nanoparticle Collisions at an Ultramicroelectrode by Electrocatalytic Amplification. *J. Am. Chem. Soc.* **2007**, *129*, 9610–9612.

(11) Sokolov, S. V.; Tschulik, K.; Batchelor-McAuley, C.; Jurkschat, K.; Compton, R. G. Reversible or Not? Distinguishing Agglomeration and Aggregation at the Nanoscale. *Anal. Chem.* **2015**, *87*, 10033–10039.

(12) Poon, J.; Batchelor-McAuley, C.; Tschulik, K.; Compton, R. G. Single Graphene Nanoplatelets: Capacitance, Potential of Zero Charge and Diffusion Coefficient. *Chem. Sci.* **2015**, *6*, 2869–2876.

(13) Plowman, B. J.; Sidhureddy, B.; Sokolov, S. V; Young, N. P.; Chen, A.; Compton, R. G. Inside Back Cover: Electrochemical Behavior of Gold--Silver Alloy Nanoparticles (ChemElectroChem 7/2016). *ChemElectroChem* **2016**, *3*, 1186.

(14) GESAMP. Sources, Fate and Effects of Microplastics in the Marine Environment: A Global Assessment. *GESAMP Reports Stud.* **2015**, *No. 90*, 98 p.

(15) Vidal, J. Microplastics Should Be Banned in Cosmetics to Save Oceans, MPs Say | Environment | The Guardian. *The Guardian*.

(16) Tanaka, K.; Takada, H.; Jambeck, J. R.; Andrady, A. L.; Eriksen, M.; Reisser, J.; Isobe, A.; Uchida, K.; Tokai, T.; Iwasaki, S.; et al. Microplastic Fragments and Microbeads in Digestive Tracts of Planktivorous Fish from Urban Coastal Waters. *Sci. Rep.* **2016**, *6*, 34351.

(17) Ellison, J.; Batchelor-McAuley, C.; Tschulik, K.; Compton, R. G. The Use of Cylindrical Micro-Wire Electrodes for Nano-Impact Experiments; Facilitating the Sub-Picomolar Detection of Single Nanoparticles. *Sensors Actuators B Chem.* **2014**, *200*, 47–52.

(18) Kätelhön, E.; Tanner, E. E. L.; Batchelor-McAuley, C.; Compton, R. G. Destructive Nano-Impacts: What Information Can Be

Extracted from Spike Shapes? *Electrochim. Acta* **2016**, *199*, 297–304.

(19) Kätelhön, E.; Feng, A.; Cheng, W.; Eloul, S.; Batchelor-McAuley, C.; Compton, R. G. Understanding Nano-Impact Current Spikes: Electrochemical Doping of Impacting Nanoparticles. *J. Phys. Chem. C* **2016**, *120*, 17029–17034.

(20) Tschulik, K.; Haddou, B.; Omanović, D.; Rees, N. V.; Compton, R. G. Coulometric Sizing of Nanoparticles: Cathodic and Anodic Impact Experiments Open Two Independent Routes to Electrochemical Sizing of Fe3O4 Nanoparticles. *Nano Res.* **2013**, *6*, 836–841.

(21) Tandon, V.; Bhagavatula, S. K.; Nelson, W. C.; Kirby, B. J. Zeta Potential and Electroosmotic Mobility in Microfluidic Devices Fabricated from Hydrophobic Polymers: 1. The Origins of Charge. *Electrophoresis* **2008**, *29*, 1092–1101.

(22) Hunter, R. J. *Zeta Potential in Colloid Science : Principles and Applications*.

(23) Neumann, C. C. M.; Laborda, E.; Tschulik, K.; Ward, K. R.; Compton, R. G. Performance of Silver Nanoparticles in the Catalysis of the Oxygen Reduction Reaction in Neutral Media: Efficiency Limitation due to Hydrogen Peroxide Escape. *Nano Res.* **2013**, *6*, 511–524.

(24) Cinková, K.; Clark, M.; Sokolov, S. V; Batchelor-McAuley, C.; Švorc, Ľ.; Compton, R. G. Improving Limits of Detection. Microdisc versus Microcylinder Electrodes. *Electroanalysis* **2016**.

(25) Kim, T.; Lim, S.; Kwon, K.; Hong, S.-H.; Qiao, W.; Rhee, C. K.; Yoon, S.-H.; Mochida, I. Electrochemical Capacitances of Well-Defined Carbon Surfaces. *Langmuir* **2006**, *22*, 9086–9088.

(26) Wehmeyer, K. R.; Wightman, R. M. Scan Rate Dependence of the Apparent Capacitance at Microvoltammetric Electrodes. *J. Electroanal. Chem. Interfacial Electrochem.* **1985**, *196*, 417–421.

(27) Gotti, G.; Evrard, D.; Fajerwerg, K.; Gros, P. Oxygen Reduction Reaction Features in Neutral Media on Glassy Carbon Electrode Functionalized by Chemically Prepared Gold Nanoparticles. *J. Solid State Electrochem.* **2016**, *20*, 1539–1550.

(28) Yang, H.-H.; McCreery, R. L. Elucidation of the Mechanism of Dioxygen Reduction on Metal-Free Carbon Electrodes. *J. Electrochem. Soc.* **2000**, *147*, 3420–3428.

(29) Michaels, A.; Bixler, H. Solubility of Gases in Polyethylene. *J. Polym. Sci* **1961**, *50*, 393–412.

(30) Emanuel, N. M.; Buchachenko, A. L. *Chemical Physics of Polymer Degradation and Stabilization (New Concepts in Polymer Science)*; CRC Press, 1987.

(31) Shao, M.; Chang, Q.; Dodelet, J.-P.; Chenitz, R. Recent Advances in Electrocatalysts for Oxygen Reduction Reaction. *Chem. Rev.* **2016**, *116*, 3594–3657.

(32) Šljukić, B.; Banks, C. E.; Compton, R. G. An Overview of the Electrochemical Reduction of Oxygen at Carbon-Based Modified Electrodes. *J. Iran. Chem. Soc.* **2005**, *2*, 1–25.

(33) Zampardi, G.; Batchelor-McAuley, C.; Kätelhön, E.; Compton, R. G. Lithium-Ion-Transfer Kinetics of Single LiMn2O4 Particles. *Angew. Chemie* **2017**, *129*, 656–659.

(34) Sokolov, S. V.; Batchelor-McAuley, C.; Tschulik, K.; Fletcher, S.; Compton, R. G. Are Nanoparticles Spherical or Quasi-Spherical? *Chem. - A Eur. J.* **2015**, *21*, 10741–10746.

(35) Szabo, A.; Cope, D. K.; Tallman, D. E.; Kovach, P. M.; Wightman, R. M. Chronoamperometric Current at

Hemicylinder and Band Microelectrodes: Theory and Experiment. *J. Electroanal. Chem. Interfacial Electrochem.* **1987**, *217*, 417–423.

(36) Stuart, E. J. E.; Zhou, Y.-G.; Rees, N. V.; Compton, R. G. Determining Unknown Concentrations of Nanoparticles: The Particle-Impact Electrochemistry of Nickel and Silver. *RSC Adv.* **2012**, *2*, 6879.

(37) Sutherland, W. A Dynamical Theory for Diffusion for Non-Electrolytes and the Molecular Mass of Albumin. *Philos. Mag.* **1905**, *9*, 781–785.

(38) Einstein, A. *Investigations on the Theory of the Brownian Movement (Republication)*; Dover Publications, 1956.